Journal of Structural Geology 130 (2020) 103893

Contents lists available at ScienceDirect

Journal of Structural Geology

journal homepage: http://www.elsevier.com/locate/jsg

The dilemma of asymmetric porphyroclast systems and sense of shear

Qing Zhang [a,*], Haakon Fossen [b]

[a] Institute of Geomechanics, Chinese Academy of Geological Sciences, Beijing, 100081, China
[b] Museum of Natural History, University of Bergen, Allégaten 41, N-5007, Bergen, Norway

ARTICLE INFO

Keywords:
Porphyroclast systems
Bookshelf structures
Mica fish
Vorticity
Sense of shear
Ductile shear zones

ABSTRACT

Asymmetric porphyroclast systems have long been used as independent shear-sense indicators based on their clast-tail asymmetry and/or stair-stepping tail geometry. Over the last two decades, advances in exploring the mechanical behavior of rigid clasts in a viscous flow has shed new light on understanding the formation of porphyroclast systems embedded in noncoaxial viscous flow and subsequently quantifying many aspects of flow kinematics. Using examples from naturally deformed rocks combined with results from recent advances, our study indicates that: (1) in general, only porphyroclast systems composed of equant-shaped clasts can be treated as independent shear-sense indicators; (2) special attention should be given to β-type porphyroclast systems composed of high-angle intermediate aspect-ratio clasts, which may contain meaningful information on bulk flow kinematics; (3) bookshelf structures cannot serve as independent shear-sense indicators. Multi-criteria and thorough three-dimensional shape analyses are suggested for a proper interpretation of flow kinematics in ductile shear zones.

1. Introduction

In ductile shear zones, relatively large and flow-resistant (rigid) minerals, typically partially recrystallized feldspar grains embedded in a fine-grained quartz-mica matrix with their mantling tails/wings composed of dynamically recrystallized quartz and mica via strain softening processes (White et al., 1980), are designated as porphyroclast systems (e.g., Passchier and Simpson, 1986) or augen structures (e.g., Vidal et al., 1980). The stair-stepping of recrystallized tails, i.e. the clast-tail asymmetry of the asymmetric porphyroclast system, has been widely used as a reliable kinematic indicator to extrapolate the shear-sense of the bulk flow of shear zones (Eisbacher, 1970; Choukroune and Lagarde, 1977; Lister and Price, 1978; Berthé et al., 1979; Simpson and Schmid, 1983; Passchier and Simpson, 1986; Hanmer and Passchier, 1991; Passchier, 1994.), although their origins are not yet fully understood (cf. Passchier et al., 1992; Passchier and Trouw, 2005; Passchier and Coelho, 2006; Griera et al., 2013; Stahr and Law, 2014). In the last two decades, a renewed and heated discussion has sprung out of two fundamental issues: Do rigid clasts rotate (e.g., Bell et al., 1992; Jiang and Williams, 2004; Johnson, 2008, 2009; Bell and Fay, 2016), and how do matrix properties impact the rotational behavior of rigid clasts in noncoaxial flow (e.g., Marques and Coelho, 2001; Mancktelow et al., 2002; Piazolo et al., 2002; ten Grotenhuis et al., 2002; Ceriani et al., 2003; Schmid and Podladchikov, 2005; Griera et al., 2011, 2013; Frieman et al., 2013; Stahr and Law, 2014; Mulchrone and Meere, 2015; Marques, 2016). These issues beg the question of whether or not clast-based kinematic criteria can be used as independent shear-sense indicators. In other words, what do these questions and related answers imply for the interpretation of flow kinematics, e.g., the impact on determining the sense of vorticity and assessing the kinematic vorticity number of the bulk flow in ductile shear zones? The goal of this study is to refine our knowledge on the kinematic significance of rigid clast rotation in a viscous matrix under general shear.

In this study, the shape characters and the sense of rotation of available rigid clasts in naturally deformed rocks, mostly from the Zhangbaling schist (Zhang et al., 2007, 2013) and published literatures, as well as matrix rheology are carefully examined; third-party criteria such as shear bands, quartz oblique fabrics, and quartz c-axis fabrics are used as independent shear-sense indicators. The validity of porphyroclast systems as independent shear-sense indicators are discussed in the light of recent advances.

2. Overview on rigid clast rotation

Early work on porhpyroclast systems and their flow kinematics was predominantly performed in the context of simple shear (e.g., Hanmer,

* Corresponding author.
E-mail address: zhan0174@umn.edu (Q. Zhang).

https://doi.org/10.1016/j.jsg.2019.103893
Received 28 June 2019; Received in revised form 26 September 2019; Accepted 26 September 2019
Available online 30 September 2019

1984; Simpson, 1986; van den Driessche and Brun, 1987; Hooper and Hatcher, 1988; Passchier and Sokoutis, 1993; ten Brink and Passchier, 1995), following the classic analytical model of Jeffery (1922) in which an isolated rigid single clast was immersed in an infinite isotropic linear viscous matrix. In Jeffery's model, the circular clast rotates synthetically at a constant rate of half of the strain rate under applied simple shear whereas the minimum and maximum rotation rates of the elliptical clast are predicted at the flow-parallel and flow-normal orientations, respectively. In the milestone analogue experiment and analytical analysis (Ghosh and Ramberg, 1976), ellipsoidal rigid clasts will reach a stable position under coupled pure and simple shear. Passchier (1987) expanded the work of Ghosh and Ramberg (1976) into a three-dimensional analytical analysis, proposing that the rotational behavior of rigid clasts in noncoaxial flow would fall into two categories if a steady monoclinic isotropic linear viscous matrix is assumed: Clasts with aspect ratios exceeding a critical value would rotate towards and stop at their stable positions; clasts with a lower aspect ratio would rotate continuously in a pulsating rate.

Questions arose regarding the validity of asymmetric porphyroclast systems as an independent shear-sense indicator when it was realized that, in several cases, a significant percentage of clasts showed evidence of rotation opposite to the bulk flow vorticity, as inferred from clast-tail asymmetry at both meso- and microscopic scales (Figs. 1 and 2). The occurrence of asymmetric porphyroclast systems with conflicting senses of rotation in naturally deformed rocks was interpreted in the light of subsimple shear (e.g., Passchier and Simpson, 1986; Passchier, 1987; Simpson and De Paor, 1993). Based on pioneering analytical results (e.g., Bobyarchick, 1986; Passchier, 1986), Simpson and De Paor (1993) turned these observations into a practical approach using the porphyroclast hyperbolic distribution analysis (PHD, De Paor, 1988; Simpson and De Paor, 1993, 1997). The significance of their work is to have the flow apophyses defined graphically, where the flow apophyses correspond to a pair of irrotational lines or planes in two-dimensional or three-dimensional plane-strain or monoclinic strain field (Passchier, 1998), oriented parallel and obliquely to the flow plane, respectively. The terms forward- and backward-rotating clasts were proposed to describe the clasts rotation in relation to the shear-sense of the bulk flow using a third-party criterion as an independent shear-sense indicator, e.g., quartz c-axis fabrics (Simpson and De Paor, 1993). Depending upon aspect ratios and initial orientations of the clasts as well as the vorticity value of the ductile flow, elliptical clasts were predicted to rotate synthetically and antithetically across the obliquely oriented irrotational lines/planes (metastable eigenvectors, Simpson and De Paor, 1993). Along with a better understanding of ductile fabrics in general shear, new structural criteria were proposed to distinguish forward- and backward-rotating clasts (Passchier, 1987; Wallis, 1995; Simpson and De Paor, 1993, 1997; Klepeis et al., 1999; Forte and Bailey, 2007) although the original purpose was to evaluate flow vorticity under subsimple shear.

The complexities of rotational behavior of rigid clasts in a viscous flow get further compounded when matrix properties are taken into consideration. Prior to the end of the last century, a simplified matrix rheology where rigid clasts are perfectly bonded to the matrix of a steady-state isotropic linear flow, was generally assumed. Bell (1985) proposed that the rigid clast in an anastomosing network of shear bands may remain stationary due to partitioning-induced zero angular velocity of the clasts (Johnson, 2008), a scenario of strain localization in the matrix and strain partitioning between the clast and viscous matrix (Aerden, 2004; Johnson, 2009); the spiral trails in and around the clast were interpreted as overprinting of foliations produced in multiphase deformation (e.g., Bell et al., 1992; Bell and Fay, 2016). Based on numerical modeling, however, Jiang and Williams (2004) challenged their conclusion, claiming that they violate physical basics of angular momentum balance. Marques and Burlini (2008) concluded that the rotation of the equant-shaped clast in a non-linear viscous flow follows Jeffery's prediction, even when matrix anisotropy such as shear bands develops around the clast during deformation. A similar conclusion was reached by Fletcher (2009), who through a mathematical approach found that the rotation rate of an elliptical clast is independent of the matrix anisotropy. On the contrary, using a crystal plasticity numerical approach, Griera et al. (2011) argued that the rotational behavior of a rigid circular clast is anisotropy dependent: The rigid clast rotation can be significantly reduced or fully stopped by the development of shear bands when high strain is attained. They also questioned if Mohr-Coulomb plasticity is an appropriate description of flow rheology, although strain-localization induced matrix anisotropy indeed results in limited rotation of the rigid clast (ten Grotenhuis et al., 2002; Fay et al., 2008).

The impact of matrix anisotropy on the rotational behavior of the rigid clast in viscous flow was also explored in terms of intrinsic fabric anisotropy (e.g., Mandal et al., 2005a; Fletcher, 2009; Dabrowski and Schmid, 2011; Griera et al., 2013; Frieman et al., 2013), i.e., a viscous matrix composed of thin layers with alternating viscosities. Results of these numerical models show that the rotation of the circular clast is always synthetic relative to the applied shear stress, although it would be reduced or even fully stopped with the increase of matrix anisotropy (e.g., Dabrowski and Schmid, 2011). However, the final asymmetric clast-tail geometry could be very complicated and easily misinterpreted

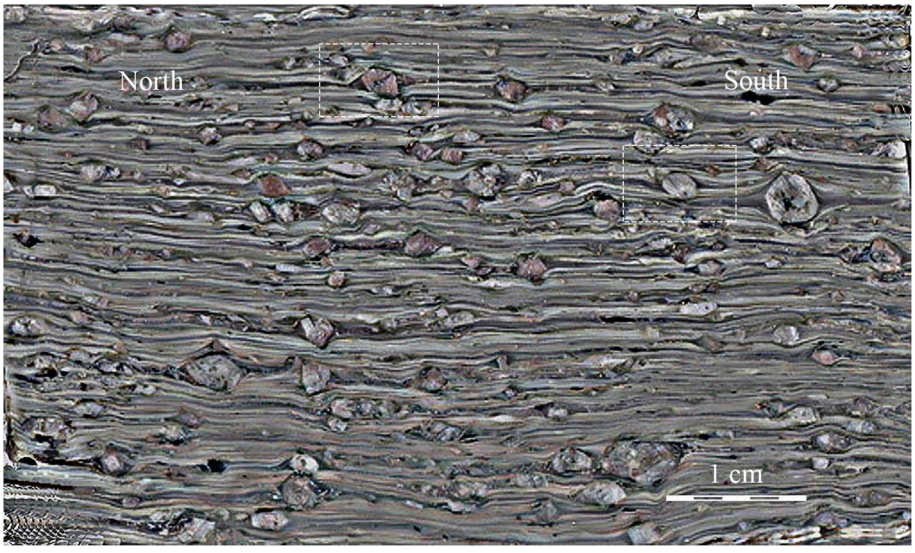

Fig. 1. Scanned image of polished rock slice of the Zhangbaling schist (XZ plane). Boxes of dashed line highlight two types of S_2 clasts. The dark- and light-color ribbons are composed of fine-grained dynamically recrystallized quartz and extremely fine-grained groundmass of plagioclase, respectively. Notice that the sense of rotation of the major clasts is top-to-north based on the clast-tail asymmetry while the sense of vorticity of the bulk flow is top-to-south, determined by shear bands, quartz c-axis, and S–C fabrics in quartz ribbons (Zhang et al., 2007).

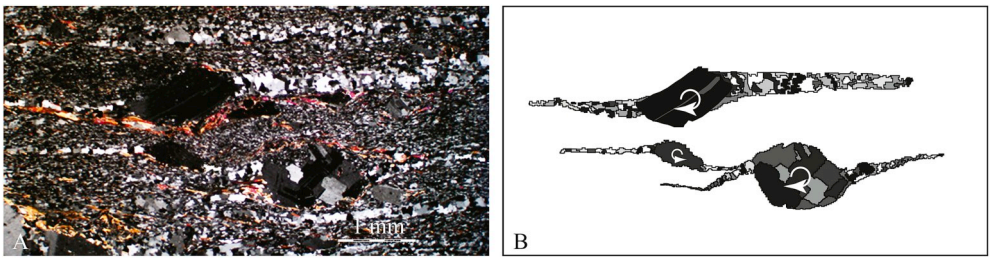

Fig. 2. A: Photomicrograph of asymmetric porphyroclast systems from the Zhangbaling schist, XZ plane, Anhui, China. B: Sketch of Fig. 2A, highlighting conflicting sense of rotation, arrows showing the sense of rotation of the clast as inferred from clast–tail asymmetry.

in terms of kinematics, particularly when the matrix anisotropy is not parallel to the shear zone boundaries (cf. Griera et al., 2013). If deformation is localized to rheologically weak layers and the size of the rigid clast is comparable to the width of these layers, a scenario of flow confinement (Marques and Cobbold, 1995; Marques and Coelho, 2001; Marques et al., 2005a, 2005b, 2014; Griera et al., 2013; Marques, 2016), the flow pattern will be significantly altered around the clast; analogue and numerical modeling show that reduced, fully inhibited, and reversed (antithetic) rotation of elliptical clasts can occur under simple shear, depending on the shape and orientation of the clast as well as the degree of flow confinement (cf. Marques et al., 2014 and references therein). In spite of the controversies around rigid clast rotation that have resulted from analytical, analogue, and numerical methods, a consensus exists that rigid clast rotation in anisotropic media is yet not fully understood (Passchier et al., 1992; Dabrowski and Schmid, 2011; Griera et al., 2013), although synthetic rotation is predicted/produced for circular clasts in these models.

Similar effects, particularly antithetic (backward) rotation and clast stabilization, were also well documented under simple shear in a series of analogue, theoretical, and numerical models (e.g., Ildefonse and Mancktelow, 1993; Marques and Coelho, 2001; Mancktelow et al., 2002; ten Grotenhuis et al., 2002; Ceriani et al., 2003; Bose and Marques, 2004; Marques and Bose, 2004; Mandal et al., 2005b; Schmid and Podladchikov, 2004, 2005; Mulchrone, 2007; Mancktelow, 2013; Marques et al., 2014; Mulchrone and Meere, 2015) in which a slipping or decoupling boundary between the clast and matrix interface was applied, mostly by introducing a weak layer to mimic the dynamically recrystallized mantle around the clast. Different from the classic models (e.g., Ghosh and Ramberg, 1976; Passchier, 1987) in which the clast is assumed to be perfectly welded to the matrix, the rate and sense of rotation of the clast in slipping/decoupling mode is considered to be determined by factors relating to the shape and orientation of the clast, thickness of the weak layer (mantle), and the viscosity contrast between the mantling layer and the matrix (e.g., Ceriani et al., 2003; Schmid and Podladchikov, 2004, 2005; Mancktelow, 2013). Marques et al. (2014) argued that the stair-stepping of the tails, depending upon the rate of mantle production (e.g., ten Brink and Passchier, 1995; Bose and Marques, 2004; Marques and Bose, 2004; Schmid and Podladchikov, 2004, 2005), is a direct expression of the degree of slipping condition and flow confinement; the maximum stair-stepping occurs in the slipping mode during confined flow via forward or backward rotation, although the backward rotation is limited in both cases. Particularly, the nearly identical σ−tails around the elliptical clasts were produced during opposite sense of rotation in their analogue experiments (Bose and Marques, 2004; Marques and Bose, 2004; Marques et al., 2014), implying that the clast-tail asymmetry may only be used as a diagnostic proof of the sense of rotation for equant-shaped clasts.

The presence of clast populations in nature generates another issue: The impact of clast interaction on the rotational behavior of the rigid clast in a viscous matrix, which has attracted considerable interest. Deviated from the classic prediction on single isolated grains (cyclic free rotation, Jeffery, 1922), a stable or metastable clast-shape fabric can be produced under simple shear via interaction between neighboring clasts (e.g., Ildefonse et al., 1992a; Tikoff and Teyssier, 1994; Arbaret et al., 1996; Piazolo et al., 2002; Jessell et al., 2009; Yamato et al., 2012) even if they are not in direct contact (e.g., Ildefonse et al., 1992b; Ildefonse and Mancktelow, 1993; Arbaret et al., 2000; Samanta et al., 2003; Mandal et al., 2005b). Regardless of the shape and initial orientation of the clasts, applied coherent vs. incoherent matrix-clast interfaces (e.g., Mandal et al., 2005b) and modeling techniques, similar conclusions were drawn from these studies: Concentration of clast populations plays a critical role on the rotational behavior of populated clasts due to the interaction, i.e., collision, tiling, and impeded rotation (e.g., Ildefonse et al., 1992a; Tikoff and Teyssier, 1994; Arbaret et al., 1996) between neighboring clasts or perturbation-induced changes in flow pattern around the clast (e.g., Ildefonse et al., 1992b; Ildefonse and Mancktelow, 1993; Samanta et al., 2003; Mandal et al., 2005b). The denser the concentration, the stronger the shape fabric, which is inclined to the shear direction at a small angle. In the case of nondirect contact (e.g., Ildefonse and Mancktelow, 1993; Mandal et al., 2005b), the rotation rate could be flow (simple vs. pure shear) and boundary-condition dependent; while clustering leads to the imbrication of two or more particles, clast rotation is significantly slowed down or prohibited. Neverthless, antithetic rotation is observed in both cases and favored by increasing concentration of clast populations. Tikoff and Teyssier (1994) pointed out that rigid clast rotation is essentially unpredictable due to the interaction (i.e., collision, tiling, and impeded rotation) between neighboring clasts before the entrained clasts get fully separated. In practical application, isolated single grain or those with spacing greater than twice the clast size is recommended for extracting kinematic information about the bulk flow to minimize the impact of clast interaction (e.g., Ildefonse et al., 1992b; Mandal et al., 2003).

When power-law material was applied to the matrix, which is considered a better approximation of natural flow rheology than the linear one (e.g., Passchier et al., 1993; ten Brink and Passchier, 1995; Masuda and Mizuno, 1996; Pennacchioni et al., 2000; Piazolo et al., 2002; Schmid and Podladchikov, 2005; Marques and Burlini, 2008; Marques et al., 2011a, 2011b; Mancktelow, 2011, 2013; Marques et al., 2014), it was considered that power-law rheology may influence the geometry of the flow pattern around clasts (Passchier et al., 1993; ten Brink and Passchier, 1995), leading to the formation of spiral tails (δ-like) wrapping around the clast. However, numerical simulations (Masuda and Mizuno, 1996; Bons et al., 1997; Pennacchioni et al., 2000) indicate that, at least for two-dimensional rigid circular objects, the effects are not drastic. In general, a stronger shape fabric will develop due to the higher stress-strain rate sensitivity in a power-law matrix (e.g., Piazolo et al., 2002). Nevertheless, an agreement appears to be achieved among researchers that there is no significant deviation of mechanical behavior of rigid clasts in a power-law flow as compared to linear flow (e.g., Masuda and Mizuno, 1996; Bons et al., 1997; Pennacchioni et al., 2000; Marques and Burlini, 2008; Xypolias, 2010; Marques et al., 2014).

When a non-steady flow matrix is assumed (Stahr and Law, 2014), which is the case of natural deformation, the sense of rigid clast rotation changes instantaneously with changes in strain rate and flow vorticity, implying that the rotational behavior of rigid clasts in non-steady flow is essentially unpredictable.

Given the complications and controversies addressed in the explorations in the last two decades, the question emerges again: To what extent can clast-based kinematic criteria be used as independent shear-sense indicators? Is it time to abandon porphyroclast systems as shear-sense indicators?

3. Rigid clast rotation in general (subsimple) shear

The two basic types of asymmetric porphyroclast systems, σ- and δ-type clasts, were first identified based on their shapes of tails/wings and clast-tail asymmetry relative to the reference frame (Hanmer, 1984; Simpson, 1986). A δ−clast system is characterized by thin wings/tails that cross the reference plane (shear plane); a σ−clast system is featured by wide wings/tails near the clast and the tails/wings extend along the same sides of the shear plane (Fig. 3). A third type of asymmetric porphyroclast was distinguished by a 'naked' clast and perturbed matrix flow without tails/wings around the clast, which is referred to as the θ clast (Hooper and Hatcher, 1988; Passchier, 1994). A fourth one was recognized by multi-generation tails/wings, a transient structure formed during the transition from a δ- to a σ-clast via progressive rotation of the clast and consecutive development of tails/wings (Passchier and Simpson, 1986; Passchier and Sokoutis, 1993). All of these contrast the symmetric φ–clasts where the tails are centered and parallel to the general foliation.

A number of factors have been attributed to the clast-tail asymmetry such as perturbed local flow pattern around the clast, the ratio between recrystallization rate of tails and rotation rate of the clast, matrix rheology (linear vs. power-law flow), viscosity contrast between tails and matrix, and the rate of mantle production. Passchier and Simpson (1986) proposed that the ratio between dynamic recrystallization rate of tails and rotation rate of the clast is one of the most important factors in determining the type of a porphyroclast system: The δ−system develops when clast rotation is relatively fast and recrystallization slow; the σ−system forms when rotation is slow relative to recrystallization, based on the result of analogue modeling in which a Newtonian matrix under simple shear is applied. This argument is corroborated by the results of the ring-shear experiment (Passchier and Sokoutis, 1993). When power-law matrix rheology was applied (Passchier et al., 1993; ten Brink and Passchier, 1995), spiral tails around the clast were produced, which leads to an alternative interpretation that the δ− and σ−type structures are merely the products of a power-law and a Newtonian matrix, respectively; stair-stepping of tails is determined by perturbation-induced changes in flow pattern (eye-shaped vs. bow-tie-shaped separatrices). Similar structures, particularly δ−type structures with tails wrapping around the clast were produced in both analogue (van den Driessche and Brun, 1987) and numerical modeling (Bons et al., 1997), in which flow field pattern rather than matrix rheology was called for as the primary factor controlling tail geometry. Regardless of controversies, it is noteworthy that the same conclusions were drawn from these studies: High shear strain is required for the formation of δ structures; isoclinal drag folds (rolling structure, van den Driessche and Brun, 1987) and even sheath folds develop at tips of the clast at high strain as reliable shear-sense indicators (e.g., van den Driessche and Brun, 1987; Passchier et al., 1993; ten Brink and Passchier, 1995; Arbaret et al., 2001; Rosas et al., 2002; Ceriani et al., 2003; Mulchrone, 2007; Dabrowski and Schmid, 2011).

From a series of analogue experiments when the clast is mantled by a low-viscosity film under simple shear (e.g., Ceriani et al., 2003; Marques and Bose, 2004), Marques and Bose demonstrated that nearly identical σ−tails can be produced when nonequant dimensional clasts experience opposite sense of rotation in response to changes in flow pattern, leading to the interpretation that the σ− and δ−tails are products of slipping and nonslipping clast-matrix interfaces, respectively, depending on the rate of mantle production. Similar conclusions were reached by Schmid and Podladchikov (2004, 2005) via numerical simulations. It has been commonly accepted that the clast-tail asymmetry is indicative of the sense of clast rotation (e.g., Simpson and Schmid, 1983; Passchier and Simpson, 1986; Hanmer and Passchier, 1991; Passchier and Trouw, 2005; Passchier and Coelho, 2006). Given the complications and controversies, it is necessary to reevaluate and justify the use of porphyroclast systems as shear-sense indicators in practical applications. In the following discussions, the term tail is used as a general term for tails and wings.

3.1. The single-grain system

As predicted by classic models (Ghosh and Ramberg, 1976; Passchier and Simpson, 1986; Passchier, 1987), equant-shaped clasts generally behave as forward-rotating 'σ' and, particularly, 'δ' systems mantled with well-developed tails at both meso- and microscopic scales under subsimple shear (Fig. 4A). Due to the spherical shape, the rotation of equant-shaped clasts is immune to the pure-shear component in non-coaxial flow, always consistent with the sense of the flow vorticity. On the other hand, clasts with high aspect ratios (approaching or exceeding the critical aspect ratio R_c, Passchier, 1987) tend to evolve into nearly symmetric σ systems, characterized by well-developed semi-symmetric tails subparallel to the shear plane and low-angle clasts (<10°) inclined both clockwise and anticlockwise with respect to the bulk flow direction

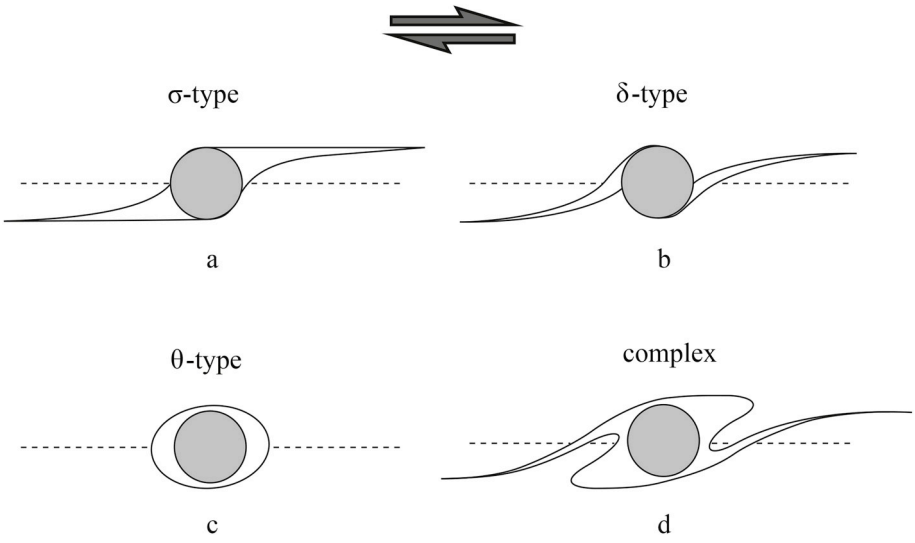

Fig. 3. Classifications of asymmetric mantled porphyroclasts, arrows show the sense of shear.

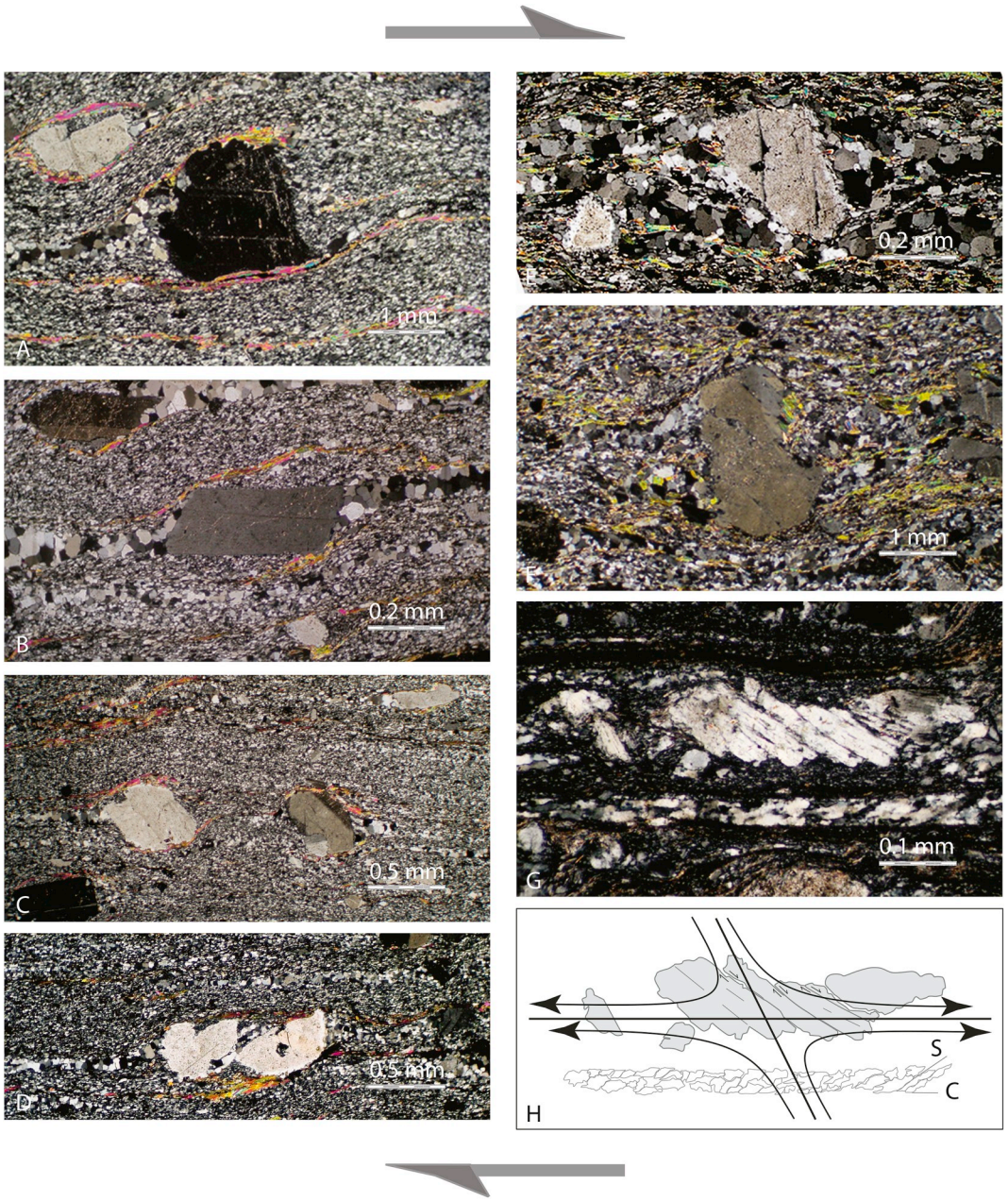

Fig. 4. Photomicrographs of the Zhangbaling schist and the Fucha Shan gneiss. Images are from the XZ planes; the sense of the vorticity, shown by the grey arrows, is determined from shear bands, quartz c-axis, and S–C fabrics in quartz ribbons. A: Equant-shaped forward-rotating δ porphyroclast. B: High-aspect-ratio porphyroclast with semisymmetrical tails, noticing the low angle between shear plane and the long axis of the clast. C: Backward-rotating σ clast. D: Forward-rotating fractured grain of plagioclase with half of δ tails. E: β clast with nearly symmetrical broad tails. F: High-angle porphyroclast with multiple tails and ambiguous sense of rotation. G: Domino-type fragmented porphyroclasts (bookshelf structure) and oblique quartz foliation from Fucha Shan gneiss, Anhui, China. H: Interpretation of the bookshelf structure in plagioclase. S and C refer to S- and C-planes marked by elongated quartz and quartz ribbons, respectively. Horizontal and vertical arrows represent simple and pure shear components. Curved arrows represent flow lines. Horizontal and oblique straight lines show stable and metastable flow eigenvectors, respectively.

(Fig. 4B).

The orientation and the sense of rotation of the clasts with intermediate aspect ratios (R = ~1.5–2.75, e.g., Xypolias, 2010; Zhang and Teyssier, 2013) are extremely sensitive to flow vorticity. Forward- and backward-rotating 'σ' grains are commonly observed in ductile shear zones (e.g., Simpson and De Paor, 1993; Klepeis et al., 1999; Forte and Bailey, 2007; Zhang and Teyssier, 2013). However, these porphyroclast systems, particularly the fully developed ones with well-defined clast--tail asymmetry, contain no kinematic information about the bulk flow. Essentially, there is no discernible geometric difference between a forward- and a backward-rotating 'σ' system (Fig. 4C and D), which can therefore be considered as mirror images. Thus, without a third-party shear-sense indicator or a thorough understanding of flow vorticity (e.g., Simpson and De Paor, 1993; Klepeis et al., 1999; Xypolias, 2010; Fossen and Cavalcante, 2017), flow kinematics based purely on the clast-tail asymmetry could easily be overinterpreted.

Efforts to better understand the flow kinematics and the rotational behavior of rigid clasts in viscous flow never ceased. Klepeis et al. (1999) identified a type of backward-rotating 'σ' clast, referred to as β_2 clasts (Fig. 5A), characterized by nearly symmetric broad tails and a high-angle antithetic orientation to the bulk flow direction, which is not commonly reported. However, shape fabric analysis of the Zhangbaling

schist (Zhang and Teyssier, 2013) revealed that the long axis of the observed β_2 clast (Fig. 4E) is parallel or subparallel to the metastable eigenvector, suggesting that the rough bilateral symmetry of the broad tails was likely produced by non-partitioned pure and simple shear components at the metastable position of the clast, which experienced the least amount of rotation or irrotation (β_2 in Fig. 5A).

Forte and Bailey (2007) expanded the discussion to the formation of porphyroclast systems with the long axis of clasts making high angles to the foliation (Fig. 5A, hereafter referred to and abbreviated as S_1 grain for convenience), postulating that the short foliation-parallel 'σ' tails were produced from inhibited growth when the clast rotated forwardly out of the metastable orientation. Likewise, a porphyroclast system characterized by antithetic orientation and fully-developed 'σ' tails (S_2 in Fig. 5A) was proposed to form through backward rotation if the long axis of the clast was originally oriented off the unstable eigenvector in the backward-rotating field. Forte and Bailey (2007) argued that these criteria can serve as credible, independent shear-sense indicators. In reality, the shape and asymmetry of the clast-tail system could be more complicated when clasts rotate passively through the foliation-normal orientation. For instance, subvertical clasts with multi-tails (Figs. 4F and 5B) were frequently observed in the Zhangbaling schist, a zone-narrowing scenario (cf. Zhang et al., 2007; Zhang et al., 2013; Zhang and Teyssier, 2013 for the Zhangbaling transpressional tectonics), in which the 'δ' tails are likely first generated when the clast rotates forwardly out of the metastable position via picking the angular velocity, then followed by developing 'σ' tails as the clast approaches the foliation-normal orientation (labeled as I and II, respectively in Fig. 5B). Finally, the 'δ' tails would be replaced by the 'σ' tails and a forward 'σ' grain with well-defined clast-tail asymmetry is expected to form in response to perturbation-induced changes in flow pattern if deformation proceeds. Fundamentally, these high-angle porphyroclast systems are transient products of rigid clast rotation, created during acceleration of the clast rotation when they sweep through the unfavored foliation-normal orientations, forming temporary multi-generation tails and wings (Passchier and Simpson, 1986; Passchier and Sokoutis, 1993). Accordingly, the formation of a forward 'δ' system of intermediate aspect ratio is likely but unnecessarily restricted in the quadrant defined by the metastable eigenvector and the bisector between the stable and metastable eigenvectors in the forward-rotating field.

3.2. Fractured grains and bookshelf structures

Fractured grains and bookshelf structures (Choukroune and Lagarde, 1977; Etchecopar, 1977), typically feldspars, are commonly observed in ductile or brittle-ductile shear zones. Strictly speaking, these structures are not conventional porphyroclast systems, as they consist of multiple grains with complex inter-clast interaction of collision, tiling, and impeded rotation (e.g., Tikoff and Teyssier, 1994; Piazolo et al., 2002; Jessell et al., 2009). However, since fractured grains and bookshelf structures retain important kinematic significance, and rigid clast rotation plays a critical role in their formation, these unconventional porphyroclast systems are included in the following discussion.

The bookshelf structure has been regarded as an independent shear-sense indicator (cf. Simpson and Schmid, 1983). Conventionally, a bookshelf structure forms as broken crystal fragments rotate in the shear direction like a collapsing set of books in a bookshelf, i.e., the microfractures and the long axes of the fractured grains become progressively more inclined towards the shear plane as shearing proceeds (Etchecopar, 1977; Simpson and Schmid, 1983). Simpson and De Paor (1993) proposed that the microfractures develop preferentially along the bisectors between the eigenvectors in noncoaxial flow where the clasts undergo the maximum angular shear; the fractured grains and the bookshelf structure were plotted (maybe not intentionally) in the forward- and backward rotating fields (Fig. 5A), respectively, in their analytical work (Simpson and De Paor, 1993). However, the probability for single- and multifractures developing in the forward- and backward-rotating fields should be the same. In the Zhangbaling schist, a pair of fractured plagioclase grains with well-developed clast-tail asymmetry was observed in the forward-rotating field (Figs. 4D and 5B); the sense of rotation of the clasts inferred from the clast-tail asymmetry (stair-stepping of the tails) is consistent with other kinematic indicators such as quartz c-axis fabrics, S–C fabrics, and shear bands (Zhang et al., 2007, 2013). Similarly, a domino-type bookshelf structure (Passchier and Trouw, 2005) in the transpressional root of the Zhangbaling belt was discovered in the backward-rotating field (Figs. 4G and 5B), using quartz c-axis and S–C fabrics as shear-sense indicators of the bulk flow (Zhang et al., 2007). The formation of this bookshelf structure was interpreted as the result of backward rotation in noncoaxial flow when the long axes of the fractured feldspars and the microfracture planes (crystal cleavage) were originally oriented shallower than the unstable eigenvector (Fig. 4H), or alternatively by stabilization of a stack of grains under the combined effects of clast interaction and flow confinement during antithetic rotation (e.g., Mandal et al., 2005b; Marques et al., 2014). Similar observations were made in recent work by Moreira and Dias (2018).

The situation could be more complicated in nature: A pair of bookshelf structures composed of oppositely dipping fractured feldspar grains and microfracture planes (Fig. 6A; note that the left-hand one is crosscut by two sets of microfractures, forming a so-called mosaic fragmented porphyroclast system according to Passchier and Trouw,

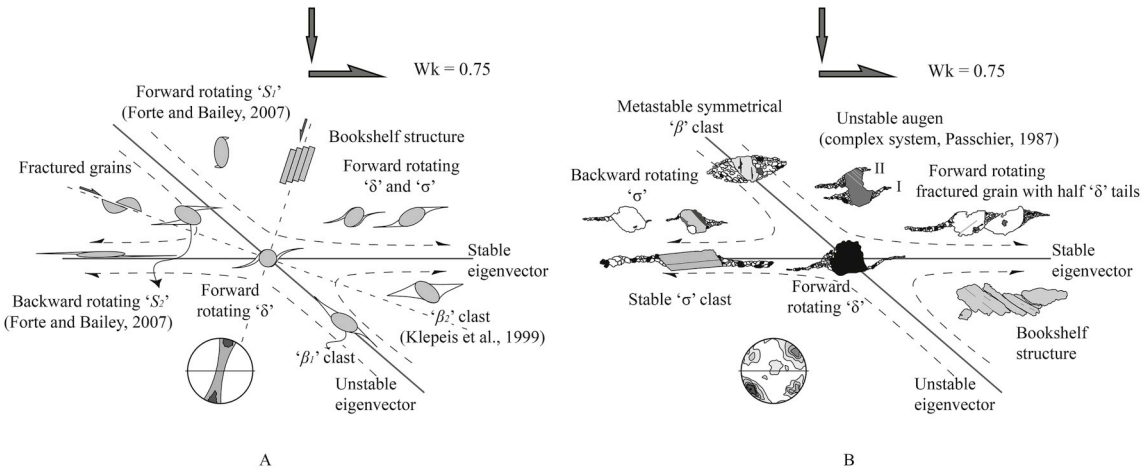

Fig. 5. A: Proposed asymmetry-based shear-sense indicators in subsimple shear, modified after Simpson and De Paor (1993). B: Asymmetric porphyroclast systems with alternative interpretations on sense of rotation of the clast, numbers next to the tail indicating sequential stages of tail development.

2005) were observed in the Ailao Shan-Red River shear zone (Tapponnier et al., 1990; Leloup et al., 1995), Yunnan, southwestern China. Clearly, it is impossible to distinguish which set of the bookshelf structures was produced via forward or backward rotation based on their geometry and inclination directions particularly if a more complex history such as multiphase deformation, or slipping clast-matrix boundary in flow confinement (note the laminated flow matrix of extremely fine-grained quartz and mica around the clasts via dynamic recrystallization) is allowed for. Similarly, a pair of bookshelf structures from a sheared dike in northeast Brazil confined in pervasively developed shear bands were disclosed (Fig. 6B). Formation of these conjugately fractured feldspar porphyroclasts can be attributed to a number of factors, such as the shape and initial orientation of the feldspar grain, vorticity value of the bulk flow, clast interaction, flow confinement, and deformation partitioning between the clast and matrix, although the sense of shear of most of the bookshelf structures in this specific case is consistent with that of the bulk flow (Fig. 6C), using shear bands and quartz c-axis fabrics as third-party shear-sense criteria. Considering the extensively developed shear bands in this rock, perturbed local flow pattern around the clasts at sample- and microscopic scales resulted from partitioned matrix-clast behavior (e.g., Marques et al., 2005a; Marques et al., 2005b; Marques et al., 2014), i.e., strain localization in the form of shear bands and restricted freedom of clast rotation between shear bands should be largely responsible for the formation of conjugate bookshelf structures in a strain-localization and -partitioning induced heterogeneous strain field. Nevertheless, fractured clasts or bookshelf imbricates can be produced by either forward or backward rotation; the use of geometry and asymmetry to extrapolate the flow kinematics is neither intuitive nor straightforward.

3.3. Mica fish

In kinematic analyses, porphyroclasts such as feldspars are generally treated as rigid objects rotating passively in a relatively weaker, viscous matrix. Obviously, the rigidity of the porphyroclast is rheology-dependent. Thus, formation of mica fish, produced predominantly by rigid body rotation and intracrystal sliding (e.g., ten Grotenhuis et al., 2003; Passchier and Trouw, 2005), can be considered in the same way as porphyroclast systems. In fact, a number of minerals, such as tourmaline (ten Grotenhuis et al., 2002), sillimanite (Pennacchioni et al., 2001; Mancktelow et al., 2002), amphibole (Mancktelow et al., 2002; Zhang et al., 2007), and hematite (Ferreira et al., 2016), behave similarly to micas in a fine-grained weak matrix, forming mineral fish characterized by their long axes oriented at a small angle to the shear plane with dynamically recrystallized minerals developing at the tips of the clast, particularly for those that are lenticular and platy in shape.

Just like asymmetric porphyroclast systems, mica fish has long been regarded as a reliable shear-sense indicator (e.g., Simpson and Schmid, 1983; Lister and Snoke, 1984; ten Grotenhuis et al., 2003; Mukherjee, 2011). However, the same problem resides in the rotational behavior of micas in micaceous quartzitic mylonites: determined by well-defined clast-tail asymmetry (Fig. 7), the sense of rotation of mica from the Ailao Shan-Red River shear zone in Diancangshan opposes the bulk sense of shear as determined by quartz S–C and c-axis fabrics, which is consistent with the regional kinematic results in previous work (e.g., Tapponnier et al., 1990; Leloup et al., 1995). A conflicting sense of rotation of mica clasts relative to the sense of the bulk flow can be interpreted in several ways: Synthetic glide on (001) planes when the cleavage plane of mica crystals are oriented at a small angle to the shear plane opposing the simple shearing flow (type 6 of ten Grotenhuis et al., 2003), antithetic rotation of lenticular mica in confined flow (e.g., Marques, 2016) or flow heterogeneity if the viscosity of the mantling material is much lower than that of the matrix (e.g., ten Grotenhuis et al., 2002; Schmid and Podladchikov, 2005), and/or backward rotation of rigid clasts under subsimple shear due to a combination of initial orientation and aspect ratios of the mica, vorticity number of the ductile flow, finite strain, etc. Nevertheless, it is reasonable to argue that mica fish, behaving as rigid clasts in a weak matrix, cannot be treated as reliable independent shear-sense indicators, regardless of their shape and orientation. Therefore, great caution must be exercised when using mica fish to extrapolate flow kinematics. The same principle should apply to the formation of other mineral fish.

4. Discussion

The role of clast shape (aspect ratios in 2D) in the rotational behavior of rigid clasts embedded in a monoclinic flow is rather straightforward: Porphyroclast systems, mostly σ-type systems, composed of high-aspect-ratio clasts ($>R_c$) reach their stable positions via forward and backward rotations, lying up- or downstream at low angles to the shear plane as predicted (e.g., Ghosh and Ramberg, 1976; Passchier, 1987). However, individuals of these porphyroclast systems with well-defined clast-tail

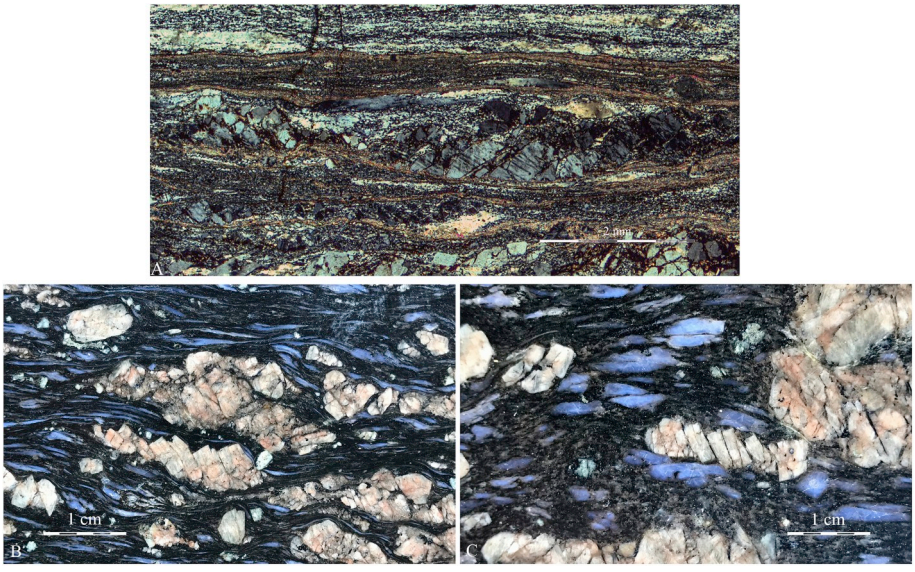

Fig. 6. A: Mosaic fragmented (left) and domino-type (right) porphyroclasts from Diancangshan, Yunnan, SE China, noticing that the left one is cross-cut by two sets of fractures. B: Conjugately fractured feldspar, and C: Domino-type porphyroclasts (bookshelf structures) from NE Brazil. Photomicrographs are from the XZ planes.

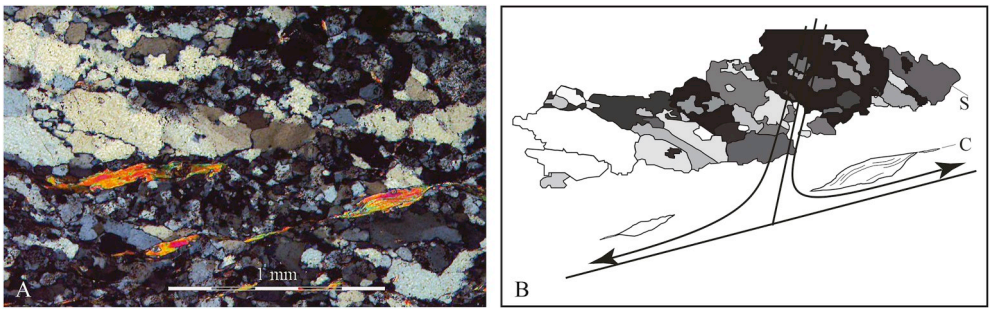

Fig. 7. Photomicrograph of mica fish and kinematic interpretation (XZ plane). A: Group 3 mica fish (ten Grotenhuis et al., 2003) from the Red River shear zone, Yunnan, China. The sense of vorticity is determined by quartz c-axis and S–C fabrics. B: Backward-rotating kinematics of the mica fish in subsimple shear.

asymmetry carry no kinematic information of the bulk flow. Strictly speaking, the pure-shear component has no effect on the rotation of equant-shaped clasts in subsimple shear, which is driven purely by the simple-shear component. Therefore, the sense of rotation of a spherical clast should reflect literally the sense of vorticity of the bulk flow. However, a porphyroclast system from the Zhangbaling schist that was composed of a subcircular clast ($R < 1.15$) (Fig. 8) was diagnosed as backward rotating determined by shear bands, quartz oblique foliation (S–C fabrics), and quartz c-axis fabric analyses (Zhang et al., 2007). This backward-rotation can be either interpreted as an apparent feature resulting from an non-optimal cut through the rock (Passchier and Williams, 1996), a complex rolling process in three dimensions (Ghosh et al., 2003; Frieman et al., 2013; Stahr and Law, 2014; Marques, 2016), or the product of backward rotation under combined effects of incoherent clast-matrix boundary and flow confinement (e.g., Marques et al., 2014; Marques, 2016). In nature, deformation is always three-dimensional whereas our observations are generally sectional. Thus, proper interpretation of deformation kinematics and flow rheology always requires a thorough three-dimensional fabric analysis.

Similarly, individual σ-type porphyroclast system made of intermediate-aspect-ratio clast with fully developed clast-tail asymmetry contains no kinematic significance. Regardless of being stabilized, i.e., under coupled pure and simple shear, flow confinement, and/or incoherent clast-matrix interface, or not, these matured fabrics (in terms of fully developed tails and clast-tail asymmetry) cannot be discriminated if they are produced by forward- or backward-rotation without a third-party criterion e.g., shear bands, quartz c-axis fabrics and oblique foliation, rolling structures, and sigmoids (Passchier and Trouw, 2005; Passchier and Coelho, 2006, Fig. 5d of Fossen and Cavalcante, 2017), although the clast-tail asymmetry or stair-stepping may truly reflect their sense of rotation. In contrast, the transient porphyroclast systems, i.e., the high-angle clasts with ambiguous, multiple tails (equivalent of the complex porphyroclast system of Passchier and Simpson, 1986 and Passchier and Sokoutis, 1993), no tails (equivalent of the θ clast of Passchier, 1994), the subvertical S_1 and back-rotating S_2 grains (Forte and Bailey, 2007), and the β grains (Figs. 5B and 9) could be kinematically important. If subsimple shear is assumed, the long axis of the β clast signifies the orientation of the instantaneous metastable flow eigenvector (Klepeis et al., 1999; Zhang and Teyssier, 2013). Thus, the β clast may retain not only information about flow kinematics but also about the kinematic vorticity number of the bulk flow, although the β_1 tails (parallel to the metastable eigenvector (Figs. 5A and 9) may only be observed in zone-widening (transtensional) deformations. Therefore, it is reasonable to argue that β and S (or Z-shaped like rolling structures and drag folds of van den Driessche and Brun, 1987) clasts, depending on the configuration of the subsimple shear flow field and the orientation of the metastable flow eigenvector (Fig. 9), are β-clast derived (referred to as β-type in Fig. 9 to honor the pioneer): When the long axis of the clasts is slightly off the metastable eigenvector no matter if it is its initial orientation, a population of β-correlated β_2-, S-, and Z-clasts will develop via forward and backward rotation. Accordingly, these β-type clasts (β-, S-, and Z-clasts) can be regarded as snapshots of the last increment of rotation of the rigid clasts in progressive deformation (Fossen et al., 2019), frozen in when the system becomes inactive. Given the nonsteady-state nature of flow rheology, a full spectrum of the β-type clasts are expected to develop from forward or backward rotation due to the oscillation of the metastable eigenvector (Stahr and Law, 2014), which will be constantly removed from the 'pool' of β-clasts (Fig. 9) as deformation proceeds. Thus, these unconventional asymmetric porphyroclasts may be treated as credible shear-sense indicators under progressive subsimple shear, although their application could be limited by their rare occurrence and structural subtleties.

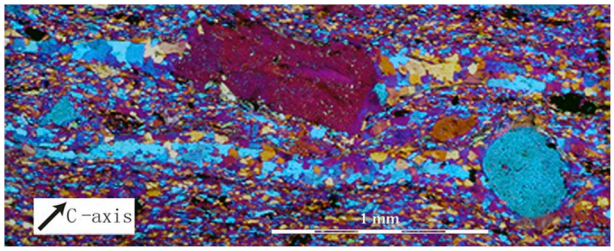

Fig. 8. Photomicrograph of the Zhangbaling schist characterized by strong quartz c-axis fabrics shown by predominant blue-colored quartz ribbons under the gypsum plate, indicating top-to-right shearing. The clast-tail asymmetry of a subcircular clast ($R < 1.15$) with well-defined clast−tail asymmetry (the other half is missing because it is found right at the edge of the thin section) at the lower right corner, suggesting top-to-left sense of rotation, Anhui, China. Crossed polars, XZ plane.

Theoretically, δ tails can be generated only at high strains in response to changes of flow pattern in the vicinity of a rigid clast (spherical or subspherical clast shape is favored) that experiences permanent synthetic rotation (cf. Passchier and Trouw, 2005; Passchier and Coelho, 2006; Xypolias, 2010 and references therein), which is widely accepted as a reliable shear-sense indicator. A 'δ' system defined by well-developed stair-stepping of recrystallized tails of quartz was detected (highlighted in the lower-right box in Fig. 1). The overall clast-tail asymmetry is comparable to a S_2 grain (upper-left box in Fig. 1); the only difference is that the latter is mantled with σ tails. Shape fabric and vorticity analyses revealed that both of them were plotted in the backward-rotating field close to the metastable eigenvector, using shear bands, quartz c-axis, and S–C fabrics in quartz ribbons as shear-sense indicators (Zhang and Teyssier, 2013; Zhang et al., 2013). However, formation of such a backward-rotating 'δ' system cannot be explained by any current analytical, numerical, or experimental model, given the fact that the path or room left for backward rotation of this rigid clast is limited for the high strains needed in a subsimple shear flow field.

Over the last couple of decades, a number of clast-based methods, i.e., the porphyroclast aspect ratio plot (PAR, a modified R_f/φ method, Passchier, 1987; Law et al., 2004), the porphyroclast hyperbolic

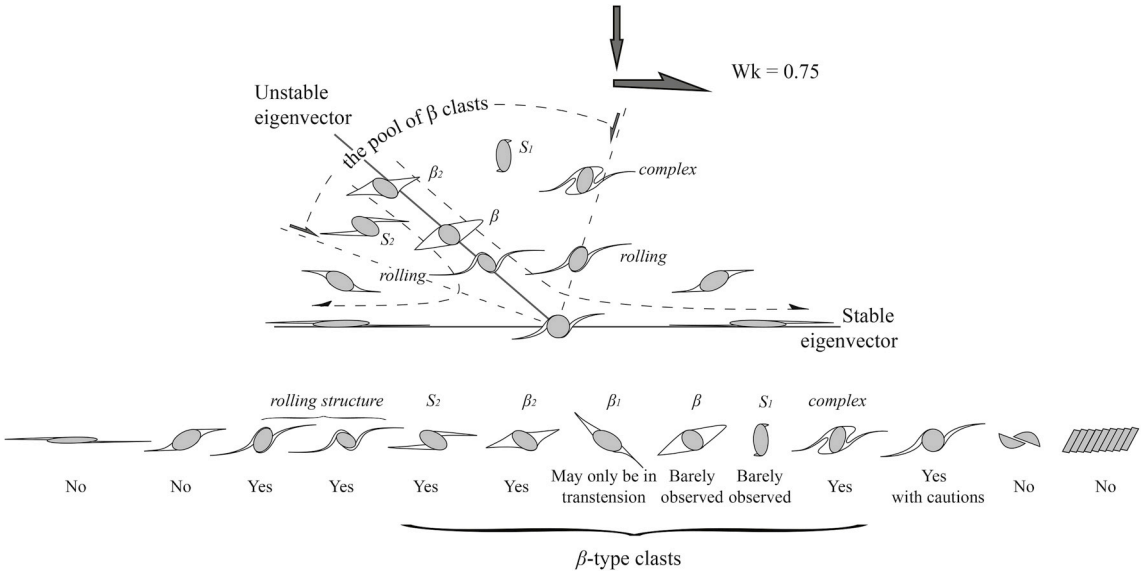

Fig. 9. Schematic presentation of possible porhyroclast systems in subsimple shear (top) and an evaluation of credibility of shear-sense indicators as discussed in the main text (bottom). Two rolling structures are presented with different shapes and clast orientations, suggesting that rolling (δ) structures are preferentially but unnecessarily developing in the quadrant defined by the metastable eigenvector and the bisector between the stable and metastable eigenvectors in the forward-rotating field.

distribution plot (PHD, Simpson and De Paor, 1993, 1997), and the rigid grain net (RGN, a unified PAR and PHD approach, Jessup et al., 2007) method have been used for estimating flow vorticity, of which the first two are the most commonly used techniques (cf. Xypolias, 2010; Fossen and Cavalcante, 2017 and references therein). Strict and idealized pre-requisites have to be met: The matrix is treated as deforming under steady-state isotropic linear monoclinic flow, although nonlinear coarse-grained matrix also behaves as a continuum (e.g., Marques and Burlini, 2008); a population of perfectly rigid clasts with a full spectrum of aspect ratios with low or no inter-clast interaction and no shape changes are perfectly bonded to the matrix under homogeneous deformation; and the strain must be large enough to allow clasts to reach their stable positions. Law et al. (2004) pointed out that a lack of high-aspect-ratio clasts leads to underestimating flow vorticity. Zhang and Teyssier (2013) reached the same conclusion, arguing that randomness and ambiguity reside inevitably in visually determining the cutoff value of R_c and locating the metastable flow eigenvector graphically due to the absence of high-aspect-ratio clasts or their low-angle orientation to the flow plane. Based on the same idealized assumptions, Li and Jiang (2011) challenged the reliability of clast-based vorticity analysis techniques, arguing that the strain required for stabilization of most clasts in a randomly oriented population is too high for natural deformation. They claimed that the reported vorticity numbers (in the range of 0.50–0.85) from naturally deformed mylonites, using clast-based shape-fabric analysis, could be reproduced in a simple-shearing flow due to the complex rotational behavior of rigid clasts in three dimensions. Similar conclusions were reached by others (e.g., Mancktelow, 2013; Stahr and Law, 2014). Stahr and Law (2014) argued further that although the 3D nature of rigid clast rotation is indeed complicated, it cannot explain the wide range of vorticity numbers (0.50–0.85) quoted by Li and Jiang (2011); reported vorticity numbers may not record either the mean kinematic vorticity number (W_m, Passchier, 1987) or that of the last flow increment for high-strain zones experiencing non-steady state progressive deformation, owing to strain-memory induced delayed clast response to the new flow field. In fact, these idealized and unrealistic assumptions are hard to justify for natural deformation. For instance, Bailey et al. (2004) pointed out that flow vorticity tends to be overestimated if the finite strain is not large enough to reorient the clasts to their stable position. On the other hand, if a slipping clast-matrix boundary is assumed, stable position can be reached under simple shear, as shown by a strong shape preferred orientation of a large population of clasts (e.g., Pennacchioni et al., 2001; Marques et al., 2007), although stabilization of clasts in high-temperature deformation could be partially attributed to the rotation of deformable passive markers (e.g., Tullis, 2002; Passchier and Trouw, 2005).

Over the last two decades, a renewed interest in rigid clast rotation embedded in a viscous matrix has emerged. Improvements on analytical methods made more sophisticated modeling, particularly numerical simulations centered on matrix rheology and fabric anisotropy, possible, regardless of modeling techniques and materials applied. Undoubtedly, results from these delicate models have shed new light on understanding the mechanical behavior of rigid clasts in a viscous flow and subsequently quantifying many aspects of flow kinematics, including vorticity analysis. Considering extensively developed shear bands, recrystallized mantle around the clast, and lamellae- or layer-controlled flow as well as densely packed clasts at sample- and microscopic scales, a general conclusion can be reached that partitioning of deformation between the clast and its matrix is extremely common and important. Accordingly, stabilization of rigid clasts in a subsimple shear flow can be achieved under lower strain and flow vorticity than those predicted by classic models (Ghosh and Ramberg, 1976; Passchier, 1987; Simpson and De Paor, 1997), caused by fabric anisotropy, clast-matrix decoupling, flow confinement, and clast interactions as discussed above. In other words, the vorticity value in naturally deformed rocks can easily be underestimated. For instance, a rigid clast may not sense the simple-shear component in cases where strain is completely partitioned between matrix and clasts. However, the following question emerges: How do we justify the applicability of clast-based method on flow vorticity estimation to natural deformation if significant strain partitioning exists?

Given the complexities associated with rigid clast rotation in nature, there is no question that exploration of the rotational behavior of rigid clasts in a viscous matrix will continue and trigger more debate and discussion. Efforts never cease.

5. Concluding remarks

In this study, the shape, orientation, and clast-tail asymmetry of

porphyroclast systems from naturally deformed rocks are carefully examined; the sense of rotation of rigid clasts is determined using a third-party shear-sense criterion, and the rheological impacts on the rotational behavior resulted from recent studies are well addressed. Our study indicates that: (1) in general, only porphyroclast systems composed of equant-shaped clasts can be treated as independent shear-sense indicators; (2) special attention should be given to β-type porphyroclast systems, which may contain meaningful information on bulk flow kinematics; (3) bookshelf structures cannot serve as independent shear-sense indicators either, and; (4) cautions must be taken when using mica fish to extrapolate flow kinematics.

Acknowledgements

This study was supported by the National Science Foundation of China (41072071; 4117218). The authors give their sincerest thanks to Christian Teyssier for many enlightening and stimulating discussions on the subject. We are thankful for helpful reviews by F. O. Marques, and P. Xypolias as well as the editorial handling by S. Laubach.

References

Aerden, D.G.A.M., 2004. Correlating deformation in variscan NW–iberia using porphyroblasts; implications for the ibero–armorican arc. J. Struct. Geol. 26, 177–196.
Arbaret, L., Diot, H., Bouchez, J.-L., 1996. Shape fabrics of particles in low concentration suspension: 2D analogue experiments and application to tiling in magma. J. Struct. Geol. 18, 941–950.
Arbaret, L., Fernandez, A., Jezek, J., Ildefonse, B., Launeau, P., Diot, H., 2000. Analogue and numerical modelling of shape fabrics: application to strain and flow determination in magmas. Trans. R. Soc. Edinb. Earth Sci. 91, 97–109.
Arbaret, L., Mancktelow, N.S., Burg, J.P., 2001. Effect of shape and orientation on rigid particle rotation and matrix deformation in simple shear flow. J. Struct. Geol. 23, 113–125.
Bailey, C.M., Francis, B.E., Fahrney, E.E., 2004. Strain and vorticity analysis of transpressional high-strain zones from the Virginia Piedmont, USA. In: Aslop, G.I., Holdsworth, R.E., McCaffrey, K.J.H., Hand, M. (Eds.), Flow Processes in Faults and Shear Zones, vol. 224. Geological Society, Special Publications, pp. 249–264.
Bell, T.H., 1985. Deformation partitioning and porphyroblast rotation in metamorphic rocks: a radical reinterpretation. J. Metamorph. Geol. 3, 109–118.
Bell, T.H., Johnson, S.E., Davis, B., Forde, A., Hayward, N., Witkins, C., 1992. Porphyroblast inclusion–trail orientation data; eppure non son girate! J. Metamorph. Geol. 10, 295–307.
Bell, T.H., Fay, C., 2016. Holistic microstructural techniques reveal synchronous and alternating and alusite and staurolite growth during three tectonic events resulted from shifting partitioning of growth vs deformation. Lithos 262, 699–712.
Berthé, D., Choukroune, P., Jegouzo, P., 1979. Orthogneiss, mylonite and noncoaxial deformation of granites: the example of the South Armorican Shear Zone. J. Struct. Geol. 1, 31–42.
Bobyarchick, A.R., 1986. The eigenvalues of steady flow in Mohr space. Tectonophysics 122, 35–51.
Bons, P.D., Barr, T.D., ten Brink, C.E., 1997. The development of δ–clasts in non-linear viscous materials: a numerical approach. Tectonophysics 270, 29–41.
Bose, S., Marques, F.O., 2004. Controls on the geometry of tails around rigid circular inclusions: insights from analogue modelling in simple shear. J. Struct. Geol. 26, 2145–2156.
Ceriani, S., Mancktelow, N.S., Pennacchioni, G., 2003. Analogue modelling of the influence of shape and particle/matrix interface lubrication on the rotational behaviour of rigid particles in simple shear. J. Struct. Geol. 25, 2005–2021.
Choukroune, P., Lagarde, J.L., 1977. Plans de schistosite et deformation rotationnelle; l'exemple du gneiss de Champtoceaux (Massif Armoricain). C. R. Hebd. Seances Acad. Sci. Ser. D Sci. Nat. 284, 2331–2334.
Dabrowski, M., Schmid, D.W., 2011. A rigid circular inclusion in an anisotropic host subject to simple shear. J. Struct. Geol. 33, 1169–1177.
De Paor, D.G., 1988. R_f/ϕ_f strain analysis using an orientation net. J. Struct. Geol. 10, 323–333.
Eisbacher, G.H., 1970. Deformation mechanics of mylonitic rocks and fractured granites in Cobequid mountains, Nova Scotia, Canada. Geol. Soc. Am. Bull. 81, 2009–2020.
Etchecopar, A., 1977. A plane kinematic model of progressive deformation in a polycrystalline aggregate. Tectonophysics 39, 121–139.
Fay, C., Bell, T.H., Hobbs, B.E., 2008. Porphyroblast rotation versus nonrotation: conflict resolution! Geology 36, 307–310.
Ferreira, F., Lagoeiro, L., Morales, L.F.G., Oliveira, C.G.D., Barbosa, P., Ávila, C., Cavalcante, G.C.G., 2016. Texture development during progressive deformation of hematite aggregates: constraints from VPSC models and naturally deformed iron oxides from Minas Gerais, Brazil. J. Struct. Geol. 90, 111–127.
Fletcher, R.C., 2009. Deformable, rigid, and inviscid elliptical inclusions in a homogeneous incompressible anisotropic viscous fluid. J. Struct. Geol. 31, 382–387.
Fossen, H., Cavalcante, G.C.G., 2017. Shear zones–A review. Earth Sci. Rev. 171, 434–455.
Fossen, H., Cavalcante, G.C.G., Pinheiro, R.V.L., Archanjod, C.J., 2019. Deformation–progressive or multiphase? J. Struct. Geol. 125, 82–99.
Forte, A.M., Bailey, C.M., 2007. Testing the utility of the porphyroclast hyperbolic distribution method of kinematic vorticity analysis. J. Struct. Geol. 29, 983–1001.
Frieman, B.M., Gerbi, C.C., Johnson, S.E., 2013. The effect of microstructural and rheological heterogeneity on porphyroblast kinematics and bulk strength in porphyroblastic schists. Tectonophysics 587, 63–78.
Ghosh, S.K., Ramberg, H., 1976. Reorientation of inclusions by combination of pure shear and simple shear. Tectonophysics 3, 1–70.
Ghosh, S.K., Sen, G., Sengupta, S., 2003. Rotation of long tectonic clasts in transpressional shear zones. J. Struct. Geol. 25, 1083–1096.
Griera, A., Bons, P.D., Jessell, M.W., Lebensohn, R.A., Evans, L., Gomez–Rivas, E., 2011. Strain localization and porphyroclast rotation. Geology 39, 275–278.
Griera, A., Llorens, M.-.G., Gomez–Rivas, E., Bons, P.D., Jessell, M.W., Evans, L.A., Lebensohn, R., 2013. Numerical modelling of porphyroclast and porphyroblast rotation in anisotropic rocks. Tectonophysics 587, 4–29.
Hanmer, S., 1984. The potential use of planar and elliptical structures as indicators of strain regime and kinematics of tectonic flow. Geol. Surv. Can. Pap. 84–1B, 133–142.
Hanmer, S., Passchier, C.W., 1991. Shear–sense indicators: a review. Geol. Surv. Can. Pap. 90, 1–71.
Hooper, R.J., Hatcher, R.D., 1988. Mylonites from the Towaliga fault zone, central Georgia: products of heterogeneous non–coaxial deformation. Tectonophysics 152, 1–17.
Ildefonse, B., Launeau, P., Bouchez, J.L., Fernandez, A., 1992. Effect of mechanical interactions on the development of shape preferred orientations: a two–dimensional experimental approach. J. Struct. Geol. 14, 73–83.
Ildefonse, B., Sokoutis, D., Mancktelow, N.S., 1992. Mechanical interactions between rigid particles in a deforming ductile matrix. Analogue experiments in simple shear flow. J. Struct. Geol. 14, 1253–1266.
Ildefonse, B., Mancktelow, N.S., 1993. Deformation around rigid particles: the influence of slip at the particle/matrix interface. Tectonophysics 221, 345–359.
Jeffery, G.B., 1922. The motion of ellipsoidal particles immersed in a viscous fluid. Proc. R. Soc. Lond. A102, 161–179.
Jessell, M.W., Bons, P.D., Griera, A., Evans, L.A., Wilson, C.J.L., 2009. A tale of two viscosities. J. Struct. Geol. 31, 719–736.
Jessup, M.L., Law, R.D., Frassi, C., 2007. The Shear-Rigid Grain Net (RGN): an alternative method for estimating mean kinematic vorticity number (Wm). J. Struct. Geol. 29, 411–421.
Jiang, D.Z., Williams, P.F., 2004. Reference frame, angular momentum, and porphyroblast. J. Struct. Geol. 26, 2211–2224.
Johnson, S.E., 2008. The effects of strain localisation and rigid–object kinematics. In: Bons, P.D., Koehn, D., Jessell, M.W. (Eds.), Microdynamics Simulation, Lecture Notes in Earth Sciences, vol. 106. Springer, Berlin, pp. 247–253. https://doi.org/10.1007/978–3–540–44793–1.
Johnson, S.E., 2009. Porphyroblast rotation and strain localization: debate settled! Geology 37, 663–666.
Klepeis, K.A., Daczko, N.R., Clarke, G.L., 1999. Kinematic vorticity and tectonic significance of superposed mylonites in a major lower crustal shear zone, northern Fiordland, New Zealand. J. Struct. Geol. 21, 1385–1405.
Law, R.D., Searle, M.P., Simpson, R.L., 2004. Strain, deformation temperature and vorticity of flow at the top of Greater Himalayan slab, Everst Massif, Tibet. J. Geol. Soc. Lond. 161, 305–320.
Li, C., Jiang, D., 2011. A critique of vorticity analysis using rigid clasts. J. Struct. Geol. 33, 203–219.
Lister, G.S., Price, G.P., 1978. Fabric development in a quartz–feldspar mylonite. Tectonophysics 49, 37–78.
Lister, G.S., Snoke, A.W., 1984. S–C mylonites. J. Struct. Geol. 6, 616–638.
Leloup, P.H., Lacassin, R., Tapponnier, P., Schärer, U., Zhong, D.L., Liu, X.C., Zhang, L.S., Ji, S.C., Trinh, P.T., 1995. The Ailao Shan–Red River shear zone (yunnan, China), tertiary transform boundary of indochina. Tectonophysics 251, 3–84.
Mancktelow, N.S., Arbaret, L., Pennacchioni, G., 2002. Experimental observations on the effect of interface slip on rotation and stabilisation of rigid particles in simple shear and a comparison with natural mylonites. J. Struct. Geol. 24, 567–585.
Mancktelow, N.S., 2013. Behaviour of an isolated rimmed elliptical inclusion in 2D slow incompressible viscous flow. J. Struct. Geol. 46, 235–254.
Mancktelow, N.S., 2011. Deformation of an elliptical inclusion in two–dimensional incompressible power–law viscous flow. J. Struct. Geol. 33, 1378–1393.
Mandal, N., Samanta, S.K., Bhattacharyya, G., Chakraborty, C., 2003. Deformation of ductile inclusions in a multiple inclusion system in pure shear. J. Struct. Geol. 25, 1359–1370.
Mandal, N., Misra, S., Samanta, S.K., 2005. Rotation of single rigid inclusions embedded in an anisotropic matrix: a theoretical study. J. Struct. Geol. 27, 731–743.
Mandal, N., Samanta, S.K., Bhattacharyya, G., Chakraborty, C., 2005. Rotation behaviour of rigid inclusions in multiple associations: insights from experimental and theoretical models. J. Struct. Geol. 27, 679–692.
Marques, F.O., Burlini, L., Burg, J.-P., 2011. Microstructure and mechanical properties of halite/coarse muscovite synthetic aggregates deformed in torsion. J. Struct. Geol. 33, 624–632.
Marques, F.G., Cobbold, P.R., 1995. Development of highly non–cylindrical folds around rigid ellipsoidal inclusions in bulk simple shear: natural examples and experimental modelling. J. Struct. Geol. 17, 589–602.
Marques, F.O., Coelho, S., 2001. Rotation of rigid elliptical cylinders in viscous simple shear flow: analogue experiments. J. Struct. Geol. 23, 609–617.

Marques, F.O., Bose, S., 2004. Influence of a permanent low–friction boundary on rotation and flow in rigid inclusion/viscous matrix systems from an analogue perspective. Tectonophysics 382, 229–245.
Marques, F.O., Taborda, R.M., Bose, S., Antunes, J.V., 2005. Effects of confinement on matrix flow around a rigid inclusion in viscous simple shear: insights from analogue and numerical modelling. J. Struct. Geol. 27, 379–396.
Marques, F.O., Taborda, R.M., Antunes, J.V., 2005. 2D rotation of rigid inclusions in confined bulk simple shear flow: a numerical study. J. Struct. Geol. 27, 2171–2180.
Marques, F.O., Schmid, D.W., Andersen, T.B., 2007. Applications of inclusion behaviour models to a major shear zone system: the Nordfjord-Sogn Detachment Zone in Western Norway. J. Struct. Geol. 29, 1622–1631.
Marques, F.O., Burlini, L., 2008. Rigid inclusions rotate in geologic materials as shown by torsion experiments. J. Struct. Geol. 30, 1368–1371.
Marques, F.O., Burlini, L., Burg, J.-P., 2011. Microstructural and mechanical effects of strong fine-grained muscovite in soft halite matrix: shear strain localization in torsion. J. Geophys. Res. B08213 https://doi.org/10.1029/2010JB008080.
Marques, F.O., Mandal, N., Taborda, R., Antunes, J., Bose, S., 2014. The behaviour of deformable and non–deformable inclusions in viscous flow. Earth Sci. Rev. 134, 16–69.
Marques, F.O., 2016. Mineral lineation produced by 3–D rotation of rigid inclusions in confined viscous simple shear. Tectonophysics 684, 92–99.
Masuda, T., Mizuno, N., 1996. Deflection of non–Newtonian simple shear flow around a rigid cylindrical body by the Finite Element Method. J. Struct. Geol. 18, 1089–1100.
Moreira, N., Dias, R., 2018. Domino structures evolution in strike–slip shear zones; the importance of the cataclastic flow. J. Struct. Geol. 110, 187–201.
Mukherjee, S., 2011. Mineral fish: their morphological classification, usefulness as shear sense indicators and genesis. Int J Earth Sci (Geol Rundsch) 100, 1303–1314. https://doi.org/10.1007/s00531–010–0535–0.
Mulchrone, K.F., 2007. An analytical solution in 2D for the motion of rigid elliptical particles with a slipping interface under a general deformation. J. Struct. Geol. 29, 950–960.
Mulchrone, K.F., Meere, P.A., 2015. Shape fabric development in rigid clast populations under pure shear: the influence of no–slip versus slip boundary conditions. Tectonophysics 659, 63–69.
Passchier, C.W., 1986. Flow in natural shear zones–the consequences of spinning flow regimes. Earth Planet. Sci. Lett. 77, 70–80.
Passchier, C.W., Simpson, C., 1986. Porphyroclast systems as kinematic indicators. J. Struct. Geol. 8, 831–843.
Passchier, C.W., 1987. Stable positions of rigid objects in non–coaxial flow–a study in vorticity analysis. J. Struct. Geol. 9, 679–690.
Passchier, C.W., Trouw, R.A.J., Zwart, H.J., Vissers, R.L.M., 1992. Porphyroblast rotation: eppur si muove? J. Metamorph. Geol. 10, 283–294.
Passchier, C.W., Sokoutis, D., 1993. Experimental modeling of mantled porphyroclasts. J. Struct. Geol. 15, 895–909.
Passchier, C.W., ten Brink, C.E., Bons, P.D., Sokoutis, D., 1993. δ objects as a gauge for stress sensitivity of strain rate in mylonites. Earth Planet. Sci. Lett. 120, 239–245.
Passchier, C.W., 1994. Mixing in flow perturbations: a model for development of mantled porphyroclasts in mylonites. J. Struct. Geol. 16, 733–736.
Passchier, C.W., Williams, P.R., 1996. Conflicting shear sense indicators in shear zones; the problem of non–ideal sections. J. Struct. Geol. 18, 1281–1284.
Passchier, C.W., 1998. Monoclinic model shear zones. J. Struct. Geol. 20, 1121–1137.
Passchier, C.W., Trouw, R.A.J., 2005. Microtectonics, second ed. Springer–Verlag, Berlin, p. 133.
Passchier, C.W., Coelho, S., 2006. An outline of shear–sense analysis in high–grade rocks. Gondwana Res. 10, 66–76.
Pennacchioni, G., Fasolo, L., Cecchi, M.M., Salasnich, L., 2000. Finite–element modelling of simple shear flow in Newtonian and non–Newtonian fluids around a circular rigid particle. J. Struct. Geol. 22, 683–692.
Pennacchioni, G., Di Toro, G., Mancktelow, N., 2001. Strain-insensitive preferred orientation of porphyroclasts in Mont Mary mylonites. J. Struct. Geol. 23, 1281–1298.
Piazolo, S., Bons, P.D., Passchier, C.W., 2002. The influence of matrix rheology and vorticity on fabric development of populations of rigid objects during plane strain deformation. Tectonophysics 351, 315–329.
Rosas, F.M., Marques, F.O., Luz, A., Coelho, S., 2002. Sheath folds formed by drag induced by rotation of rigid inclusions in viscous simple shear flow: nature and experiment. J. Struct. Geol. 24, 45–55.
Samanta, S.K., Mandal, N., Chakraborty, C., 2003. Flow patterns around rigid inclusions in a multiple inclusion system undergoing bulk simple shear deformation. J. Struct. Geol. 25, 209–221.
Schmid, D.W., Podladchikov, Y.Y., 2004. Are isolated stable rigid clasts in shear zones equivalent to voids? Tectonophysics 384, 233–242.
Schmid, D.W., Podladchikov, Y.Y., 2005. Mantled porphyroclast gauges. J. Struct. Geol. 27, 571–585.
Simpson, C., 1986. Determination of movement sense in mylonites. J. Geol. Educ. 7, 246–261.
Simpson, C., De Paor, D.G., 1993. Strain and kinematic analysis in general shear zones. J. Struct. Geol. 15, 1–20.
Simpson, C., De Paor, D.G., 1997. Practical analysis of general shear zones using porphyroclast hyperbolic distribution method: an example from the Scandinavian Caledonides. In: Sengupta, S. (Ed.), Evolution of Geological Structures in Micro– to Macro–Scales. Springer, Dordrecht, pp. 169–184.
Simpson, C., Schmid, S.M., 1983. An evaluation of criteria to deduce the sense of movement in sheared rocks. Geol. Soc. Am. Bull. 94, 1281–1288.
Stahr III, D.W., Law, R.D., 2014. Strain memory of 2D and 3D rigid inclusion populations in viscous flows–What is clast SPO telling us? J. Struct. Geol. 68, 347–363.
Tapponnier, P., Lacassin, R., Leloup, P.H., Scharer, U., Zhong, D.L., Wu, H.W., Liu, X.H., Ji, S.C., Zhang, L.S., Zhong, J.Y., 1990. The Ailao Shan/Red River metamorphic belt: tertiary left–lateral shear between Indochina and South China. Nature 343, 431–437.
ten Brink, C.E., Passchier, C.W., 1995. Modelling of mantled porphyroclasts using non-Newtonian rock analogue materials. J. Struct. Geol. 17, 131–146.
ten Grotenhuis, S.M., Passchier, C.W., Bons, P.D., 2002. The influence of strain localisation on the rotation behaviour of rigid objects in experimental shear zones. J. Struct. Geol. 24, 485–499.
ten Grotenhuis, S.M., Trouwc, R.A.J., Passchier, C.W., 2003. Evolution of mica fish in mylonitic rocks. Tectonophysics 372, 1–21.
Tikoff, B., Teyssier, C., 1994. Strain and fabric analyses based on porphyroclast interation. J. Struct. Geol. 16, 477–491.
Tullis, J., 2002. Deformation of granitic rocks: experimental studies and natural examples. Rev. Mineral. Geochem. 51, 51–95.
van den Driessche, J., Brun, J.-P., 1987. Rolling structures at large shear strain. J. Struct. Geol. 9, 691–704.
Vidal, J.-L., Kubin, L., Debat, P., Soula, J.C., 1980. Deformation and dynamic recrystallization of K feldspar augen in orthogneiss from Montagne Noire, Occitania, southern France. Lithos 13, 247–255.
Wallis, S.R., 1995. Vorticity analysis and recognition of ductile extension in the Sanbagawa belt, SW Japan. J. Struct. Geol. 17, 1077–1093.
White, S.H., Burrows, S.E., Carreras, J., Shaw, N.D., Humphreys, F.J., 1980. On mylonites in ductile shear zones. J. Struct. Geol. 2, 175–188.
Xypolias, P., 2010. Vorticity analysis in shear zones: a review of methods and applications. J. Struct. Geol. 32, 2072–2092.
Yamato, P., Tartèse, R., Duretz, T., May, D.A., 2012. Numerical modelling of magma transport in dykes. Tectonophysics 526–529, 97–109.
Zhang, Q., Teyssier, C., Dunlap, J., Zhu, G., 2007. Oblique collision between north and south China recorded in zhangbaling and Fucha Shan (dabie –sulu transfer zone). In: Till, A.B., Roeske, S.M., Sample, J.C., Foster, D.A. (Eds.), Exhumation Associated with Continental Strike–Slip Fault Systems, vol. 434, pp. 167–206 of Geological Society of America Special Paper.
Zhang, Q., Teyssier, C., 2013. Flow vorticity in Zhangbaling transpressional attachment zone, SE China. J. Struct. Geol. 48, 72–84.
Zhang, Q., Giorgis, S., Teyssier, C., 2013. Finite strain analysis of the Zhangbaling metamorphic belt, SE China–Crustal thinning in transpression. J. Struct. Geol. 49, 13–22.